

Near-linear Scaling in DMRG-based Tailored Coupled Clusters: An Implementation of DLPNO-TCCSD and DLPNO-TCCSD(T)

Jakub Lang,^{1,2,*} Andrej Antalík,^{1,3,†} Libor Veis,^{1,‡} Jan Brandejs,^{1,3,§} Jiří Brabec,^{1,¶} Örs Legeza,^{4,**} and Jiří Pittner^{1,††}

¹*J. Heyrovský Institute of Physical Chemistry, Academy of Sciences of the Czech Republic, v.v.i., Dolejškova 3, 18223 Prague 8, Czech Republic*

²*Faculty of Sciences, Charles University, Albertov 6, 128 00 Praha 2, Czech Republic*

³*Faculty of Mathematics and Physics, Charles University, Ke Karlovu 3, 12116, Prague 2, Czech Republic*

⁴*Strongly Correlated Systems "Lendület" Research group,*

Wigner Research Centre for Physics, H-1525, Budapest, Hungary

(Dated: April 15, 2020)

We present a new implementation of density matrix renormalization group based tailored coupled clusters method (TCCSD), which employs the domain-based local pair natural orbital approach (DLPNO). Compared to the previous local pair natural orbital (LPNO) version of the method, the new implementation is more accurate, offers more favorable scaling and provides more consistent behavior across the variety of systems. On top of the singles and doubles, we include the perturbative triples correction (T), which is able to retrieve even more dynamic correlation. The methods were tested on three systems: tetramethylethane, oxo-Mn(Salen) and Iron(II)-porphyrin model. The first two were revisited to assess the performance with respect to LPNO-TCCSD. For oxo-Mn(Salen), we retrieved between 99.8–99.9% of the total canonical correlation energy which is the improvement of 0.2% over the LPNO version in less than 63% of the total LPNO runtime. Similar results were obtained for Iron(II)-porphyrin. When the perturbative triples correction was employed, irrespective of the active space size or system, the obtained energy differences between two spin states were within the chemical accuracy of 1 kcal/mol using the default DLPNO settings.

I. INTRODUCTION

Since its introduction to quantum chemistry¹, the coupled cluster (CC) approach has become one of the most widely used methods for the accurate calculations of dynamic correlation. It offers numerous favorable properties, such as compact description of the wave function, size-extensivity, invariance to rotations within occupied or virtual orbital subspaces and also a systematic hierarchy of approximations converging towards the full configuration interaction (FCI) limit². For instance, the CCSD(T) method³, which includes connected single-, double- and perturbative triple excitations, is notorious referred to as the gold standard of quantum chemistry².

Although the CC method performs well for single reference molecules, it becomes fairly inaccurate or breaks down completely for systems with strongly correlated electrons. Such systems are multireference in nature since they include quasi-degenerate frontier orbitals. This situation is common during dissociation processes, in diradicals, or compounds containing transition metals. Over the years, numerous efforts to generalize the CC ansatz and thus overcome this drawback gave rise to a broad family of multireference CC methods (MRCC)^{4–6}.

A possible approach for including static correlation in the CC scheme is to employ a different method like complete active space self-consistent field (CASSCF) or multireference configuration interaction (MRCI) in order to extract the information about the most important excitations^{7–29}. The retrieved information can then be introduced to a CC calculation as an external correction. One of such methods is tailored CC with single and double excitations (TCCSD)

proposed by Kinoshita et al.¹⁴, which draws on the split-amplitude ansatz by Piecuch et al.¹⁸, in which the cluster operator corresponding to single and double excitations is split into two parts. The active part is imported from a complete active space configuration interaction (CAS-CI) and kept fixed, while the external amplitudes are iterated using the standard CCSD framework. We recently extended this approach by using the density matrix renormalization group (DMRG) method to obtain the active space amplitudes^{30,31}. Related externally corrected CC approaches employ fixed T_3 and T_4 amplitudes obtained from *MRCI*³² or from stochastic CI³³ and iterate all singles and doubles in their presence. Compared to TCC, this has the advantage that the active space T_1 and T_2 can reflect the dynamic correlation outside of the active space, but one pays the price of much larger number of the T_3 and T_4 amplitudes involved.

The DMRG method, which originated in solid-state physics^{34–36}, is nowadays well established in quantum chemistry for the treatment of strongly correlated systems^{37–45}. As a numerical approximation to FCI, it can handle significantly larger active spaces compared to the conventional methods. However, even then the prohibitive scaling does not allow to include dynamic correlation and it is therefore necessary to employ some "post-DMRG" procedure. Many different attempts has been made to tackle this limitation for example with the complete active space perturbation theory (CASPT2)⁴⁶, Cholesky decomposition n-electron valence state perturbation theory (NEVPT2)⁴⁷, MRCI using cumulant reconstruction with internal contraction of DMRG wave function⁴⁸, canonical transformation⁴⁹, matrix product state (MPS) based formulation of multireference perturbation theory⁵⁰, DMRG pair-density func-

tional theory⁵¹, and also our aforementioned CC tailored by MPS wave functions (DMRG-TCCSD)^{30,52,53}.

Even though the DMRG-TCCSD method offers a reasonably efficient treatment of both static and dynamic correlation⁵⁴, its application to larger systems is hampered by the unfavorable scaling of the CCSD part of the calculation. With such a steep scaling, even massive parallelization is not sufficient to make the method applicable to molecules with hundreds of atoms. To overcome this issue, Pulay proposed to exploit the locality of the electron correlation^{55,56}. Due to its short range character for non-metallic systems, it is possible to take advantage of sparsity of the Hamiltonian matrix by employing the basis of localized orbitals.

Although the occupied orbital space can be easily localized using a variety of appropriate methods⁵⁷⁻⁵⁹, for the virtual space things get slightly more complicated. In their first works on locality, Pulay and Sæbø used projected atomic orbitals (PAOs)^{60,61}, which were also used by Werner and Schütz in the local CC method⁶²⁻⁶⁶. In this approach, each localized occupied orbital is assigned a domain of PAOs obtained by projecting out the occupied orbital components from atomic orbitals. The pairs of occupied orbitals are subsequently classified according to their real space distance and treated at either coupled cluster level (strong pairs), perturbative level (weak and distant pairs), or neglected altogether (very distant pairs).

Another idea how to make use of locality is based on the concept of dividing a large system into smaller segments and performing the calculations on each of these subsystems separately. Among such approaches belong the divide-expand-consolidate method^{67,68}, the divide-and-conquer method⁶⁹, the incremental method⁷⁰, the local natural orbital method⁷¹, and the fragment molecular orbital method⁷². The closely related cluster-in-molecule method⁷³ is based on energy decomposition into contributions corresponding to individual occupied orbitals.

Possibly the most effective way of virtual space truncation is, however, the use of pair natural orbitals (PNOs), which are known to provide compact parametrization of the virtual space. They were first used in the 1960s by Edmiston and Kraus⁷⁴ and later by Meyer⁷⁵⁻⁷⁹, Ahlrichs and Kutzelnigg^{80,81}. For many years, the progress in the area of PNO-based methods stalled, until their revival in 2009, when the new local pair natural orbital (LPNO) variants of CEPA and CCSD methods were introduced by Neese et al⁸²⁻⁸⁵. The cornerstone of this approach, the idea to use PNOs in combination with localized occupied orbitals, was later developed into the more advanced domain based local pair natural orbital (DLPNO) methods⁸⁶⁻⁸⁹.

In these, PNOs were expressed as a linear combination of PAOs in a pair-domain, which ultimately removed the bottleneck of previous PNO methods and achieved genuine linear scaling. For instance, the resulting DLPNO-CCSD method is applicable to systems with hundreds of atoms and thousands of basis functions, which renders the prior SCF calculation possibly computationally more demanding than the actual correlation treatment.

Moreover, the PNO-based approaches possess many de-

sirable properties, which allow them to be used in black box fashion. They provide a very compact description of the virtual space, which makes it computationally feasible to use sufficiently large domains of PAOs; something that would be too costly for a purely PAO-based approach. They use a limited number of cut-off parameters, which do not involve any real space distance and the calculated correlation energy smoothly depends on the values of these parameters.

Currently, PNO-based methods are developed in a number of groups including Werner⁹⁰⁻⁹³ and Hättig⁹⁴⁻⁹⁶ and are widely employed in the context of various systems of chemical interest⁹⁷⁻¹⁰⁶. Apart from single-reference methods, the methodology was also successfully applied to multireference CC techniques¹⁰⁷⁻¹¹⁰.

In this article, we build upon the previous investigation of our LPNO-TCCSD method¹¹¹ and introduce the newly implemented DLPNO-TCCSD and DLPNO-TCCSD(T) methods. Based on our experience, we revisit the molecule of tetramethylethane (TME) and address the drawbacks of the former method. The performance of the new approximation is then assessed using two benchmark systems, namely, oxo-Mn(Salen) and a model of Fe(II)-porphyrins (FeP).

II. THEORY AND IMPLEMENTATION

A. DMRG-based Tailored Coupled Clusters

The tailored coupled cluster method¹⁴, which belongs to the class of externally corrected methods, employs the split-amplitude wave function ansatz proposed by Piecuch et al.¹⁸

$$|\Psi_{\text{TCC}}\rangle = e^T |\Phi_0\rangle = e^{T_{\text{ext}} + T_{\text{CAS}}} |\Phi_0\rangle = e^{T_{\text{ext}}} e^{T_{\text{CAS}}} |\Phi_0\rangle, \quad (1)$$

where $|\Phi_0\rangle$ is the reference wave function and the cluster operator T is split into two parts: T_{CAS} which contains the active amplitudes obtained from an external calculation and T_{ext} which contains the external amplitudes i.e. the amplitudes with at least one index outside the CAS space. Another way to justify this ansatz is the formulation of CC equations based on excitation subalgebras recently introduced by Kowalski^{112,113}.

In our implementation, we employed the DMRG method to obtain the active amplitudes. Using the DMRG algorithm we first optimize the wave function, which is provided in the MPS form

$$|\Psi_{\text{MPS}}\rangle = \sum_{\{\alpha\}} \mathbf{A}^{\alpha_1} \mathbf{A}^{\alpha_2} \dots \mathbf{A}^{\alpha_k} |\alpha_1 \alpha_2 \dots \alpha_k\rangle, \quad (2)$$

where $\alpha \in \{|-\rangle, |\downarrow\rangle, |\uparrow\rangle, |\downarrow\uparrow\rangle\}$ and \mathbf{A}^{α_i} are MPS matrices. These are then contracted to obtain CI coefficients for single and double excitations $C^{114,115}$. Using the intermediate normalization and the relations between CI and CC

coefficients

$$T_{\text{CAS}}^{(1)} = C^{(1)}, \quad (3)$$

$$T_{\text{CAS}}^{(2)} = C^{(2)} - \frac{1}{2}[C^{(1)}]^2, \quad (4)$$

we are able to acquire the respective CC amplitudes, which are subsequently introduced into the CC calculation. At this point, these active amplitudes are kept frozen, while the remaining amplitudes in T_{ext} are optimized by solving the equations

$$\langle \Phi_i^a | H e^{T_{\text{ext}}} e^{T_{\text{CAS}}} | \Phi_0 \rangle_c = 0 \quad \{i, a\} \notin \text{CAS} \quad (5)$$

$$\langle \Phi_{ij}^{ab} | H e^{T_{\text{ext}}} e^{T_{\text{CAS}}} | \Phi_0 \rangle_c = 0 \quad \{i, j, a, b\} \notin \text{CAS} \quad (6)$$

analogously to the standard CCSD equations. This way, the active amplitudes account for static correlation and by optimizing the external amplitudes, we are able to recover the remaining dynamic correlation. The effect of dynamic correlation on T_{CAS} is neglected, which is an approximation inherent in the TCC method.

Due to the two-body Hamiltonian, TCC recovers the DMRG energy for $T_{\text{ext}} = 0$. In the limit of CAS including all orbitals, FCI energy is recovered, although the TCC energy does not behave monotonously when extending the CAS space⁵³. Nevertheless, in practice the optimal CAS size related to the energy minimum can be determined with low cost DMRG calculations⁵³. In addition, a quadratic error bound valid for DMRG-TCC methods is also derived⁵³.

On top of the TCCSD routine, the perturbative triples correction can be applied¹⁵. However, in order to prevent the double counting of static correlation, it is necessary to omit the terms that include the active amplitudes. This can be straightforwardly achieved by setting all active single and double amplitudes to zero during the calculation of the (T) correction.

B. Domain Local Pair Natural Orbital Approximation for TCCSD

The presented method is based on the open-shell DLPNO-CCSD code as implemented in ORCA¹¹⁶. In this section, we briefly outline DLPNO-CCSD and describe the modifications that were made to accommodate the tailored version of the method.

As in all PNO-based local methods, the whole process starts with the localization of the occupied orbitals. Based on our previous experience¹¹¹, we opt for the split-localization scheme, where the orbitals are separately localized within four distinct orbital subspaces: doubly occupied external, doubly occupied active, singly occupied active and active virtual. Such choice has been shown to provide a set of orbitals which yields a reasonable convergence behavior of the DMRG procedure¹¹⁷, without influencing the DMRG energy.

The next step is the construction of orbital domains. Using the idea of Werner et al.^{118,119}, we first construct PAOs

$$|\tilde{\mu}\rangle = \left(1 - \sum_i |i\rangle\langle i|\right) |\mu\rangle \quad (7)$$

by projecting out the localized occupied and active orbitals $|i\rangle$ from the original set of atomic orbitals $|\mu\rangle$. The acquired orbitals are subsequently normalized and the orbital domains are constructed based on the differential overlap integrals

$$(\text{DOI})_{i\mu} = \sqrt{\int_{\mathbb{R}^3} |\phi_i|^2 |\phi_{\tilde{\mu}}|^2 d^3r} \quad (8)$$

between PAOs and the set of occupied and active orbitals. Here, the first prescreening parameter comes into play – for a given occupied orbital i , only PAOs for which $(\text{DOI})_{i\mu} > T_{\text{CutDO}}$ are included within its domain. Also, if an atom contains at least one PAO, all PAOs belonging to this atom are considered for further domain construction.

At this point, the main difference of the TCC approach compared to the conventional DLPNO-CCSD is that all active indices including the active virtuals are formally treated as singly occupied. This means that during the creation of domains they share the same domain. Moreover, in the following dipole prescreening, it is ensured that every active occupied pair (i.e. a pair with both active indices) automatically survives the dipole prescreening.

After the prescreenings, unrestricted MP2 pair energies $\varepsilon_{ij}^{\text{PAO}}$ are calculated and used to categorize occupied orbital pairs ij into three classes, based on the preset cut-off parameters. Specifically, the active pairs and the pairs with energies larger than T_{CutPairs} are classified as strong, while the rest is either weak or neglected according to a related parameter. The whole process is executed in two consecutive steps. First, a crude screening is performed in smaller domains using loose thresholds, followed by the second screening in which the strong and weak pairs are again distributed between the three categories, but this time with finer thresholds. The strong pairs are then passed to the next stage, while the remaining pair energies are stored as a correction to the final energy

$$\Delta E_{\text{CutPairs}} = \sum_{ij}^{\text{weak}} \varepsilon_{ij}^{\text{PAO}} + \sum_{ip}^{\text{weak}} \varepsilon_{ip}^{\text{PAO}} + \sum_{pq}^{\text{weak}} \varepsilon_{pq}^{\text{PAO}}, \quad (9)$$

where i, j are indices of doubly and p, q of singly occupied orbitals. If the perturbative triples correction is invoked, the final weak pairs with energies higher than $0.01 \cdot T_{\text{CutPairs}}$ are also saved for later use.

Afterwards, using the non-redundant PAOs, the NEVPT2 pair densities \mathbf{D}^{ij} are constructed for the surviving pairs which do not contain any explicit information about the tailored CAS space. These are diagonalized to obtain PNO expansions \mathbf{d}^{ij} , which are then truncated based on the cut-off parameter T_{CutPNO} . Only PNOs with occupation numbers larger than its value are kept and the remaining orbitals are discarded. The final PAO/PNO transformation matrix for a given pair is then obtained by enlarging the former transformation matrix by a unit matrix

$$\mathbf{S}^{ij} = \mathbf{I}_{N_{\text{CAS}}} \oplus \mathbf{d}^{ij}, \quad (10)$$

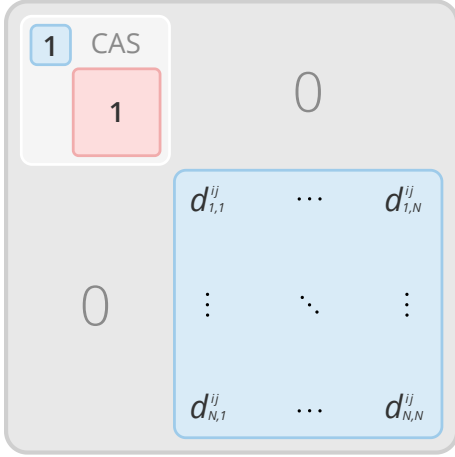


FIG. 1: An illustration of the PAO/PNO transformation matrix for an active pair ij in DLPNO-TCC. The original transformation matrix \mathbf{d}^{ij} , with N being the number of PNOs, is enlarged by an identity matrix of size N_{CAS} , which is formally composed of two blocks corresponding to singly occupied (blue) and virtual orbitals (red) included in the active space.

where N_{CAS} is the number of active SOMOs and virtual orbitals, see Figure 1. While this artificially increases the final number of PNOs, it barely increases the computational time. Singles PNOs are obtained in the same manner from the densities which are computed as

$$\mathbf{D}^{pp} = \mathbf{t}_{pp}^{(1)\dagger} \mathbf{t}_{pp}^{(1)}, \quad (11)$$

where the amplitudes are

$$\mathbf{t}_{pp}^{(1)} = \sum_{\tilde{\mu}_{pp}\tilde{\nu}_{pp}} \frac{\langle p\tilde{\mu}_{pp} || p\tilde{\nu}_{pp} \rangle}{2f_{pp} - \varepsilon_{\tilde{\mu}_{pp}} - \varepsilon_{\tilde{\nu}_{pp}}}, \quad (12)$$

where f_{pp} are diagonal Fock matrix elements. Furthermore, the pair energies are recalculated in the new truncated PNO basis and the differences between them and the original MP2 estimates in the PAO basis

$$\begin{aligned} \Delta E_{\text{CutPNO}} &= \sum_{ij}^{\text{strong}} (\varepsilon_{ij}^{\text{PAO}} - \varepsilon_{ij}^{\text{PNO}}) \\ &+ \sum_{ip}^{\text{strong}} (\varepsilon_{ip}^{\text{PAO}} - \varepsilon_{ip}^{\text{PNO}}) \\ &+ \sum_{pq}^{\text{strong}} (\varepsilon_{pq}^{\text{PAO}} - \varepsilon_{pq}^{\text{PNO}}), \end{aligned} \quad (13)$$

are stored as a correction to the final energy.

The resulting equations for singly excited amplitudes (5) now become

$$\langle \Phi_{\bar{i}} | H e^{\bar{T}_{\text{ext}}^{(1)} + \bar{T}_{\text{ext}}^{(2)}} e^{T_{\text{CAS}}} | \Phi_0 \rangle_c = 0 \quad \{i, a\} \notin \text{CAS}, \quad (14)$$

where the barred index \bar{a} indicates PNO basis. Similarly, the equations for doubly excited amplitudes (6) become

$$\langle \Phi_{\bar{i}\bar{j}} | H e^{\bar{T}_{\text{ext}}^{(1)} + \bar{T}_{\text{ext}}^{(2)}} e^{T_{\text{CAS}}} | \Phi_0 \rangle_c = 0 \quad \{i, j, a, b\} \notin \text{CAS}. \quad (15)$$

Once these equations are solved, the stored corrections (9) and (13) are added to the acquired energy. Except the fact that the active amplitudes are ‘frozen’ during the CCSD iterations, these equations are identical to single-reference DLPNO-CCSD as implemented in ORCA⁸⁹.

C. Perturbative triples correction to DLPNO-TCCSD

To calculate the triples correction using the DLPNO approach^{120,121}, it is first necessary to identify relevant compact parameterization of virtual space for every triple ijk . Domains for these triples are created as a union of i , j and k domains and the ij , jk and ik pair densities are created within these triples domains.

Next, the triples densities are constructed by averaging over the respective pair densities

$$\mathbf{D}^{ijk} = \frac{1}{3} (\mathbf{D}^{ij} + \mathbf{D}^{jk} + \mathbf{D}^{ik}), \quad (16)$$

where the triple ijk is composed either of three strong pairs or of two strong and a weak pair, as it has been previously shown that using only the strong pairs is insufficient¹²⁰. Since the amplitudes for weak pairs are not known prior to the triples calculation, the approximate MP2 amplitudes are used. The process then continues analogously to the construction of PNOs in CCSD.

Once the densities are constructed, they are diagonalized in order to obtain the triple natural orbitals (TNO) and their corresponding natural occupation numbers. The TNO expansion is then truncated based on the occupation numbers and the cut-off parameter T_{CutTNO} and from the orbitals that passed the screening a transformation matrix is formed. This matrix is enlarged by a unit matrix of dimension N_{CAS} and its final form is used to transform the integrals, amplitudes and subsequently to calculate the energy correction. As in the canonical version of the method, all active single and double amplitudes are set to zero during the calculation of the correction to prevent double-counting.

III. COMPUTATIONAL DETAILS

The DMRG calculations were performed by the Budapest QC-DMRG code¹²². The DLPNO-TCCSD and DLPNO-TCCSD(T) methods were implemented in the ORCA program package¹¹⁶, which was also used to prepare the orbitals.

Prior to DMRG calculations, we split-localized the orbitals by the Pipek-Mezey method⁵⁸ in the following orbital subspaces: internal, active doubly occupied, active singly occupied and active virtual. Orbital ordering was

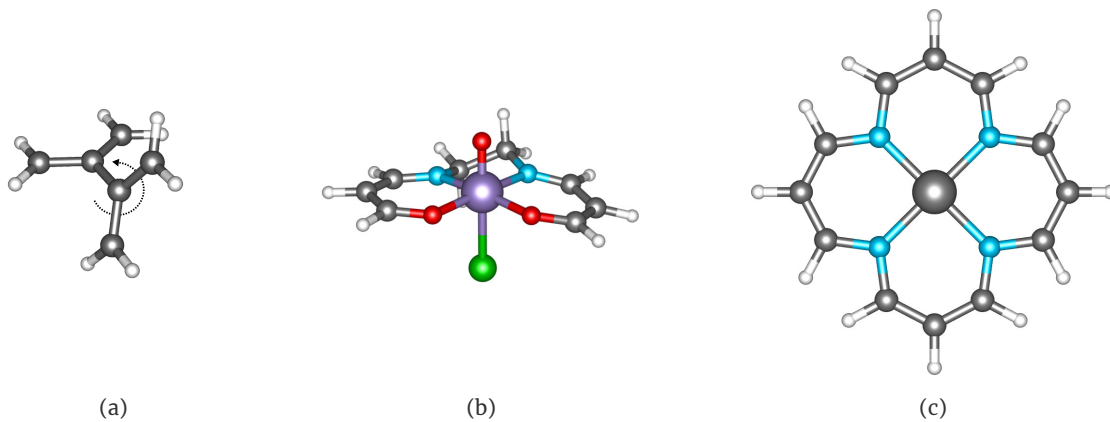


FIG. 2: Dihedral rotation of tetramethyleneethane (a), a molecule of oxo-Mn(Salen) (b) and the model of Fe(II)-porphyrin (c). Color key: iron (gray, large), manganese (violet), chlorine (green), oxygen (red), nitrogen (blue), carbon (gray, small), hydrogen (white).

subsequently optimized using the Fiedler method^{123,124} combined with minor manual adjustments. All DMRG runs were initialized by the CI-DEAS procedure^{44,125} and employed the dynamical block state selection (DBSS) procedure^{39,126} to control the accuracy of the calculation, with the truncation error criterion set to 10^{-6} . The convergence threshold was set to energy difference between two subsequent sweeps smaller than 10^{-6} a.u.

The core electrons were kept frozen throughout all coupled cluster calculations. The default set of DLPNO cut-off parameters $T_{\text{CutPNO}} = 3.33 \cdot 10^{-7}$, $T_{\text{CutPairs}} = 10^{-4}$, $T_{\text{CutMKN}} = 10^{-3}$ and $T_{\text{CutDO}} = 10^{-2}$ was employed unless otherwise stated. The other settings, referred to as TightPNO, were used for production runs: $T_{\text{CutPNO}} = 10^{-7}$, $T_{\text{CutPairs}} = 10^{-5}$, $T_{\text{CutMKN}} = 10^{-3}$ and $T_{\text{CutDO}} = 5.0 \cdot 10^{-3}$. For perturbative triples the default value of relevant cut-off parameter is $T_{\text{CutTNO}} = 10^{-9}$ for both sets of settings. To estimate the dependence of DLPNO-TCCSD energies on these parameters, one parameter was varied with remaining parameters fixed to the default value. We assess the amount of retrieved correlation energy by DLPNO approach with reference to the DMRG-TCCSD energy calculated with the canonical TCCSD implementation.

For TME, we used CASPT2(6,6)/cc-pVTZ geometries for seven values of the dihedral angle from our previous work⁵⁴. The orbitals were prepared by CASSCF(6,6) calculation with the active space containing six $2p_z$ orbitals on carbon atoms. The cc-pV6Z/C auxiliary basis set was used for the resolution of the identity (RI) approximation¹²⁷.

For oxo-Mn(Salen), we used the singlet CASSCF(10,10)/6-31G* optimized geometry by Ivanic et al.¹²⁸. The orbitals were optimized using the DMRG-CASSCF method¹²⁹⁻¹³¹ in Dunning's cc-pVXZ $X \in \{D, T, Q\}$ basis sets¹³²⁻¹³⁴. The optimization was carried out with fixed bond dimension $M = 1024$ for the smaller CAS(28,22) and $M = 2048$ for CAS(28,27). The composition of these active spaces is discussed further in detail in the paper¹¹¹. The cc-pVQZ/C auxiliary basis set

was used for RI¹³⁵.

Finally, the calculations on FeP were performed at the triplet geometry from the previous study of Li Manni and Alavi¹³⁶, with CASSCF/def2-SVP orbitals, for three distinct active spaces, which were selected based on the entanglement analysis. For the largest CAS the DMRG-CASSCF was applied, with the fixed bond dimension $M = 1024$. The def2-SVP and def2-TZVP basis sets¹³⁷ were used with the def2-TZVPP/C auxiliary basis set¹³⁸ for RI.

IV. RESULTS AND DISCUSSION

A. Tetramethyleneethane

Although small, the tetramethyleneethane molecule is a challenging system due to its complex electronic structure. To correctly describe the character of its singlet state, one needs to employ a theory with a balanced description of both static and dynamic correlation combined with a reasonably large basis set. This is the reason, why it often serves as a benchmark system for multireference methods^{54,107,139-142}. We previously studied the system with the canonical DMRG-TCCSD method⁵⁴, as well as with its LPNO version¹¹¹. In the latter, we encountered an issue with different accuracy for singlet and triplet states, which we attributed to the neglect of some terms in the LPNO-CCSD implementation in ORCA. For this reason, we revisit the system to investigate the improvement by the new DLPNO method, which should offer more robust approximation.

We performed calculations in seven different geometries corresponding to the rotation about the central C-C bond of the molecule (see Figure 2a) and different values of the cut-off parameters. These benchmarks were performed only for T_{CutPairs} and T_{CutPNO} parameters, since T_{CutDO} does not affect the results, unless an extremely small value is chosen. This behavior corresponds with the observations from previous studies^{89,109,110}.

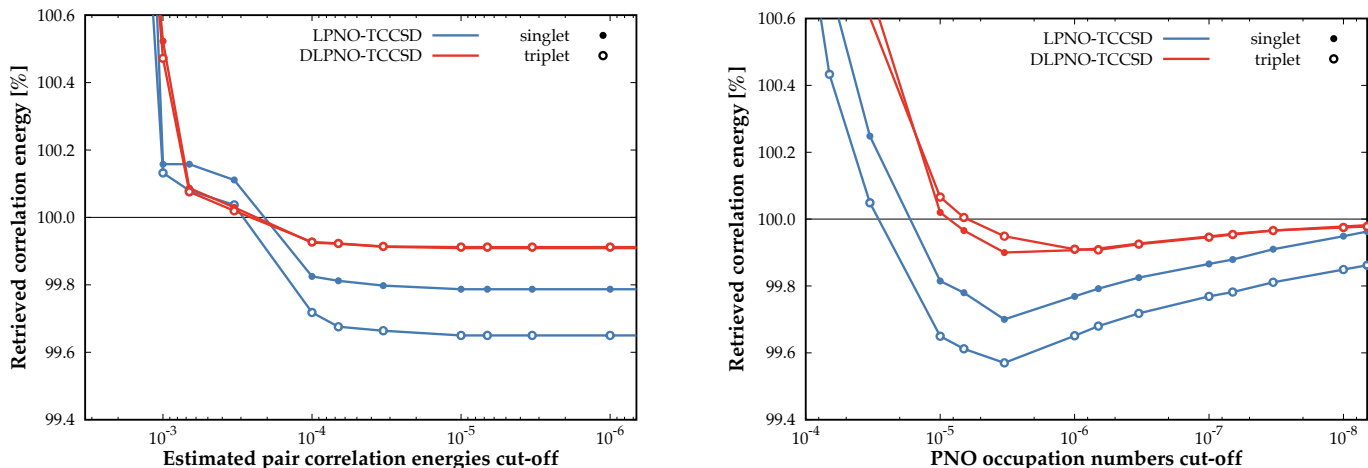


FIG. 3: The percentage of correlation energy of TME in cc-pVTZ basis retrieved by LPNO-TCCSD and DLPNO-TCCSD with respect to canonical TCCSD calculations as a function of cut-off for estimated pair correlation energies T_{CutPairs} (left) and PNO occupation numbers T_{CutPNO} (right). The plotted values are averages over the set of all geometries.

The left plot in Figure 3 shows the dependence of retrieved canonical correlation energy with respect to estimated pair correlation energies cut-off T_{CutPairs} averaged over the geometries. Both methods converge in a similar fashion, but DLPNO-TCCSD recovers 0.1–0.3% more correlation energy than LPNO-TCCSD. The right plot in the same figure shows the dependence on the second cut-off parameter, that is PNO occupation number T_{CutPNO} , which is again averaged over the geometries. Here, the DLPNO-TCCSD shows noticeably faster convergence to the canonical value compared to LPNO-TCCSD, with more accurate correlation energies even for higher values of the parameter. For instance, when the default values are used, DLPNO-TCCSD extracts over 99.91% of the canonical correlation energy.

One can notice the aforementioned discrepancy in accuracy for LPNO-TCCSD method, which can be explained by the neglected terms in the UHF-LPNO formalism. DLPNO-TCCSD does not exhibit this behavior and describes both spin states equally well. This means that the difference of the recovered correlation energy is less than 0.01% compared to LPNO-TCCSD, for which this percentage is an order of magnitude worse.

Figure 4 shows the dependence of non-parallelity error (NPE) on T_{CutPNO} for both LPNO and DLPNO version of TCCSD. It can be seen that the NPE is no larger than 0.17 kcal/mol for either spin state, with very similar value for TightPNO settings, as well as for the LPNO version.

From the chemical point of view, the most interesting property is the behavior of the singlet-triplet gap with respect to the cut-off parameters. It can be observed from the presented data that this property is well described at the default and even looser settings, which means that it can be calculated by DLPNO-TCCSD with virtually no loss in accuracy.

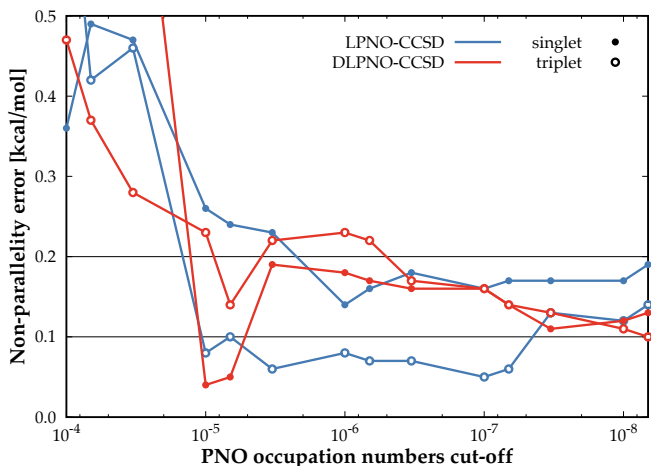


FIG. 4: Non-parallelity error for TME in cc-pVTZ as a function of cut-off for PNO occupation numbers T_{CutPNO} .

B. oxo-Mn(Salen)

The oxo-Mn(Salen) molecule (Figure 2b) has been a subject of numerous computational studies motivated mainly by its role in catalysis of the enantioselective epoxidation of unfunctional olefines^{143,144}. Due to its closely lying singlet and triplet states it is also considered to be a challenging system even for multireference methods. Over the years, many multireference studies have been published^{128,145,146}, some of which employed the DMRG method^{117,147,148} and DMRG results with dynamic correlation treatment were presented as well^{30,111,149}. This includes our previous studies, in which we used the system as a benchmark for the predecessors of the current method, namely DMRG-TCCSD and its LPNO version.

Again, we first assessed the percentage of the recovered

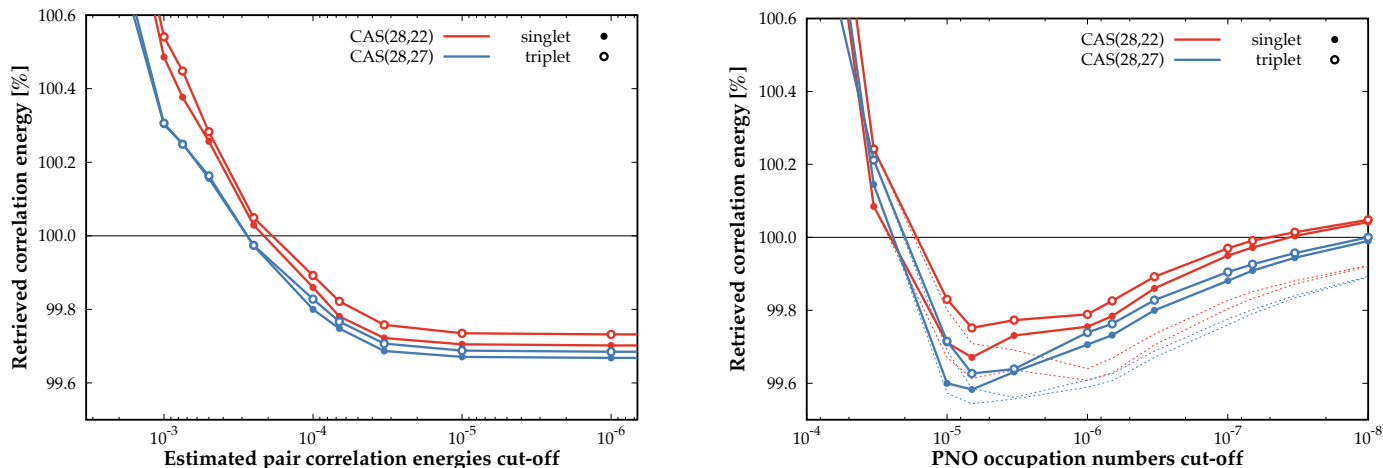


FIG. 5: The percentage of correlation energy of oxo-Mn(Salen) in cc-pVDZ basis retrieved by DLPNO-TCCSD with respect to canonical TCCSD calculations as a function of cut-off for estimated pair correlation energies T_{CutPairs} (left) and cut-off for PNO occupation numbers T_{CutPNO} (right). The thin dashed lines in the right plot represent the values for $T_{\text{CutPairs}} = 10^{-5}$.

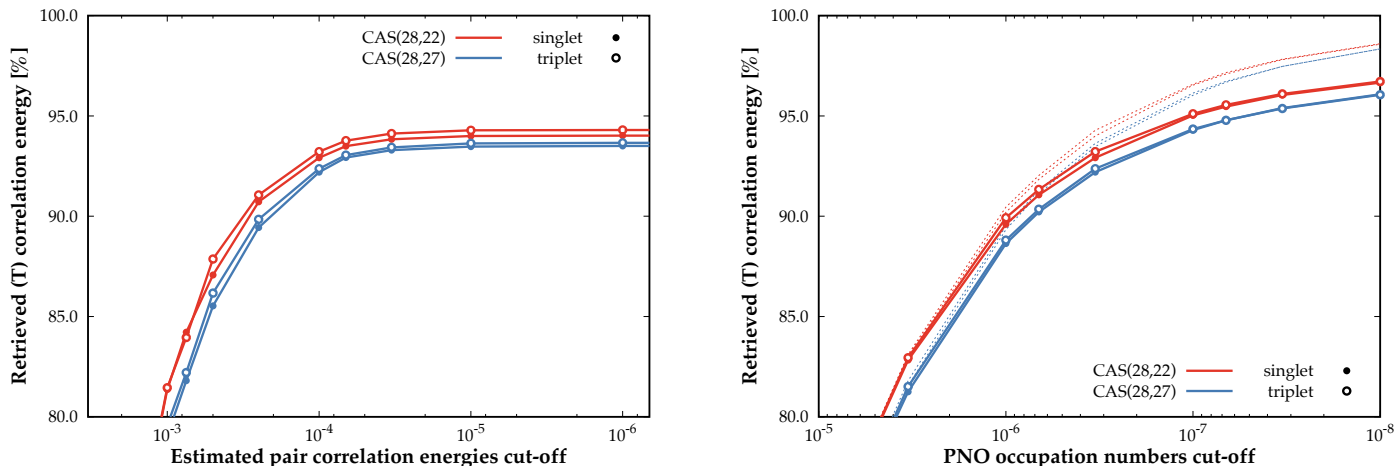


FIG. 6: The percentage of perturbative triples correction correlation energy of oxo-Mn(Salen) in cc-pVDZ basis retrieved by DLPNO-TCCSD(T) with respect to canonical TCCSD(T) calculations as a function of cut-off for estimated pair correlation energies T_{CutPairs} (left) and cut-off for PNO occupation numbers T_{CutPNO} (right). The thin dashed lines in the right plot represent the values for $T_{\text{CutPairs}} = 10^{-5}$.

canonical TCCSD correlation energy with respect to the cut-off parameter T_{CutPairs} . The curve shown in the left plot of Figure 5 follows the same trend as for TME and quickly converges. This means that the retrieved correlation energy is already converged by the value $T_{\text{CutPairs}} = 10^{-5}$. Even though the correlation energy is not yet stable for the default value 10^{-4} , the difference in accuracy between two spin states is minimal. Since we are interested in the width of the singlet-triplet gap, it appears that even this setting provides quite reasonable accuracy.

The right plot of Figure 5 shows the dependence on the cut-off parameter T_{CutPNO} . These curves smoothly near towards 100% as the parameter tightens, the behavior as observed for conventional DLPNO-CCSD. However, the energies overshoot for the very conservative values of the pa-

rameter, which is caused by overcompensation of the neglected pairs with the MP2 pair energy. For this reason, we calculated the same dependence also with the tighter setting of $T_{\text{CutPairs}} = 10^{-5}$ (the thinner dotted lines in the plot). Since for this value the correlation energies are basically converged with respect to T_{CutPairs} , we can observe that the curves now smoothly converge towards 100%. The singlet-triplet gap seems reasonably accurate for the default value of T_{CutPNO} and for more conservative values the difference in accuracy completely disappears.

We also examined the effect of these cut-offs on the perturbative triples correction recovered by DLPNO-TCCSD(T), which are shown in Figure 6. At the default value of T_{CutPairs} the energies seem to be almost converged and are fully converged at the TightPNO setting, the ac-

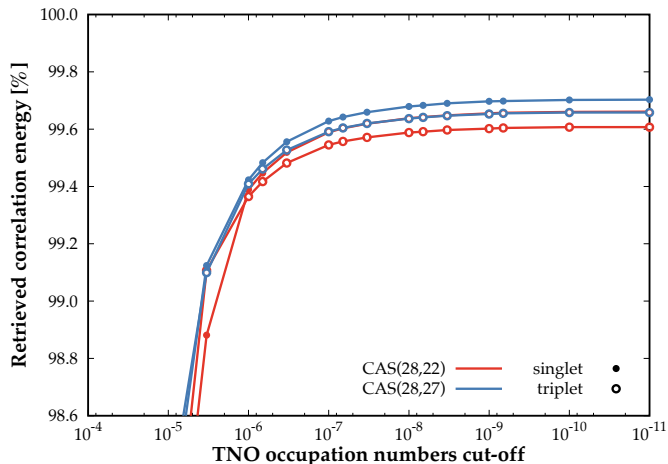


FIG. 7: The percentage of correlation energy of oxo-Mn(Salen) in cc-pVDZ basis retrieved by DLPNO-TCCSD(T) with respect to canonical TCCSD(T) calculations as a function of cut-off for TNO occupation numbers T_{CutTNO} .

TABLE I: Energy differences in kcal/mol between DLPNO-TCCSD and DLPNO-CCSD(T) calculations with different settings of cut-off parameters and equivalent canonical calculations on oxo-Mn(Salen) in cc-pVDZ.

		CAS(28,22)		CAS(28,27)	
		default	TightPNO	default	TightPNO
SD	S	2.52	3.45	3.60	4.30
	T	1.92	3.01	3.06	3.97
	$\Delta E_{\text{S-T}}$	0.60	0.44	0.54	0.33
SD(T)	S	6.38	5.30	7.33	6.19
	T	5.54	4.79	6.67	5.80
	$\Delta E_{\text{S-T}}$	0.84	0.51	0.66	0.39

tually relevant relative accuracy does not change. In case of T_{CutPNO} , the curves seem to slowly converge towards 100%, which is even more apparent when tighter cut-off on pair energies is in place. Note, that these values represent only the percentage of the canonical triples correction not the total correlation energy and for this particular system, the triples correction amounts to less than 3% of the total correlation energy. On top of that, we investigated the sensitivity of overall correlation energy on the T_{CutTNO} with the conclusion that the default value is more than adequate, see Figure 7.

Table I contains the differences between DLPNO and canonical energies for the singlet-triplet gap. Although the errors in energies for singlet or triplet state alone are substantial (especially for the larger CAS), the errors for the gap are well within the chemical accuracy of 1 kcal/mol. When the perturbative triples correction is invoked, tighter cut-offs are preferable. The same can be observed in Figure 8, where the chemical accuracy is achieved even with looser than default settings. Also the behavior of the DLPNO ap-

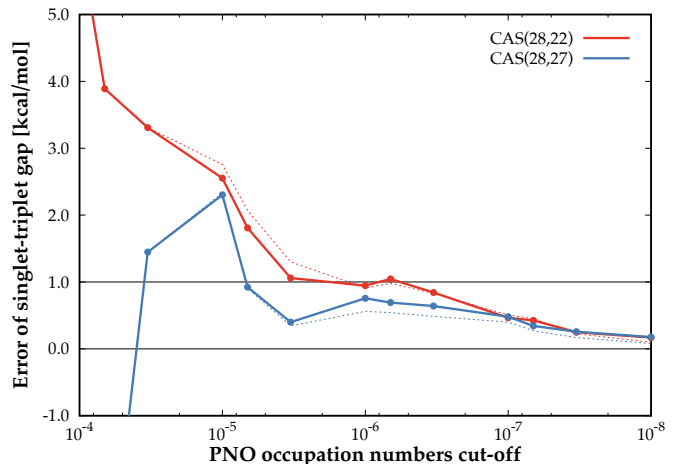


FIG. 8: The error of DLPNO-TCCSD(T) in singlet-triplet gap of oxo-Mn(Salen) in cc-pVDZ basis with respect to canonical TCCSD(T) calculations as a function of cut-off for PNO occupation numbers T_{CutPNO} . The thin dashed lines represent the values for $T_{\text{CutPairs}} = 10^{-5}$.

TABLE II: The singlet and triplet energies of oxo-Mn(salen) in cc-pVXZ basis sets. the difference $E(^1\text{A}) - E(^3\text{A})$ in kcal/mol. Results for different active spaces and in various basis sets.

	DZ	TZ	QZ
LPNO-TCCSD(28,22) ¹¹¹	6.2	6.3	6.3
DLPNO-TCCSD(28,22)	6.9	7.3	6.9
DLPNO-TCCSD(T)(28,22)	5.9	6.3	5.8
LPNO-TCCSD(28,27) ¹¹¹	3.7	3.1	2.9
DLPNO-TCCSD(28,27)	4.1	4.0	3.1
DLPNO-TCCSD(T)(28,27)	4.0	5.0	2.9
NEVPT2(28,22) ¹⁴⁹	-7.4	1.6	2.4

proximation seems quite stable with respect to the size of the active space.

When we compare these results to the previous LPNO-CCSD calculations¹¹¹, the DLPNO-TCCSD has smaller error in absolute energies, but larger in gaps. This can be attributed to the rather fortunate cancellation of errors in the LPNO case, but otherwise the DLPNO implementation is more reliable due to smaller errors in absolute energies and smooth convergence towards the canonical correlation energies.

Moreover, we performed calculations with up to cc-pVQZ basis set. We found the results to be consistent with the previous LPNO-TCCSD calculations and NEVPT2(28,22), with perturbative triples correction being responsible only for a minor shift in energy, see Table II. Even though the calculation in cc-pVQZ, which amounts to 1178 basis functions, is perfectly within the possibilities of the LPNO approach, it took 60% longer to finish under the same conditions (8 cores, 30GB of memory per core) compared to the DLPNO calculation.

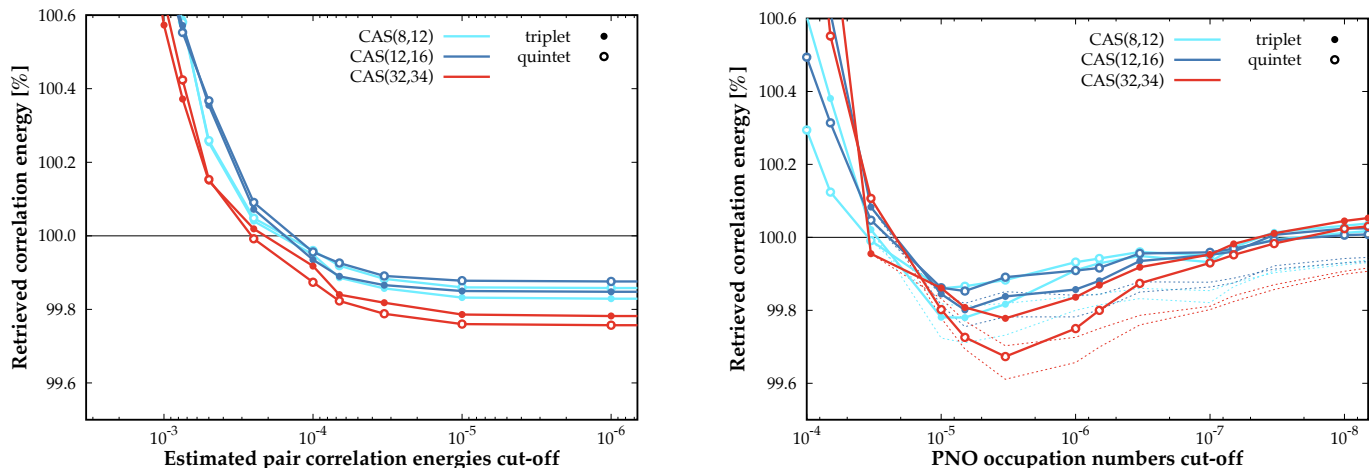


FIG. 9: The percentage of correlation energy of FeP in def2-SVP basis retrieved by DLPNO-TCCSD with respect to canonical TCCSD calculations as a function of cut-off for estimated pair correlation energies T_{CutPairs} (left) and cut-off for PNO occupation numbers T_{CutPNO} (right). The thin dashed lines in the right plot represent the values for $T_{\text{CutPairs}} = 10^{-5}$.

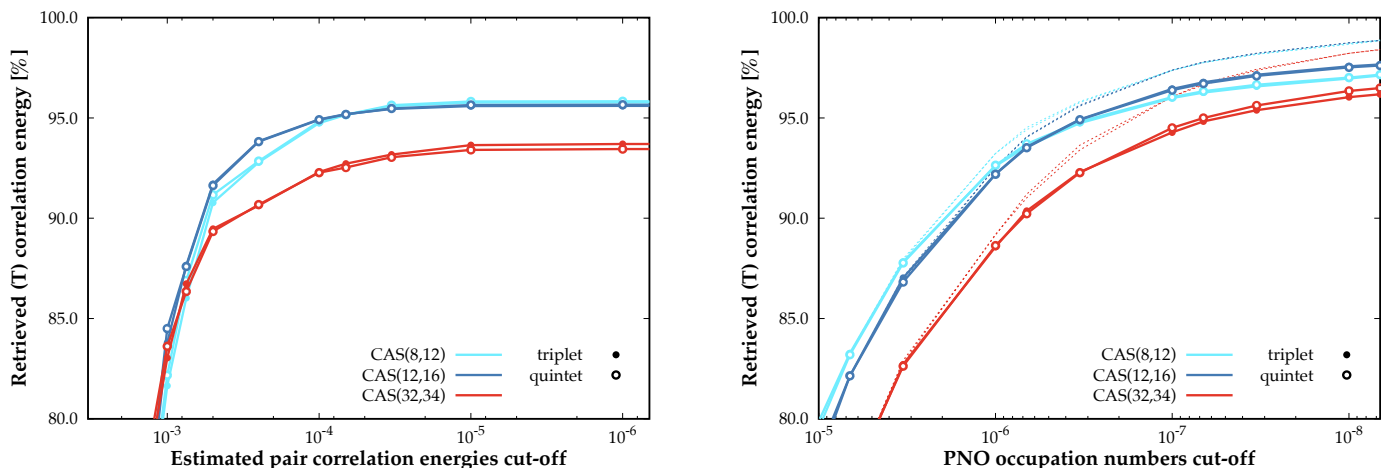


FIG. 10: The percentage of perturbative triples correction correlation energy of FeP in def2-SVP basis retrieved by DLPNO-TCCSD(T) with respect to canonical TCCSD(T) calculations as a function of cut-off for estimated pair correlation energies T_{CutPairs} (left) and cut-off for PNO occupation numbers T_{CutPNO} (right). The thin dashed lines in the right plot represent the values for $T_{\text{CutPairs}} = 10^{-5}$.

C. Iron(II) Porphyrin Model

Fe(II) porphyrin derivatives play important roles in reactions related to material science and biological processes due to their closely lying spin states. The chosen model has previously been a subject of several large scale CASSCF studies^{136,150} and we therefore consider it to be an interesting system to test the efficiency of the method for several active spaces of different size.

The left plot in Figure 9 shows the dependence on the T_{CutPairs} cut-off parameter. As for oxo-Mn(Salen), the curves converge smoothly and at 10^{-5} they are practically converged. The accuracy is consistent for triplet and quintet spin states and it differs maximally by 0.05% of the retrieved canonical correlation energy. This is true regard-

less of the size of the active space, although the overall accuracy is slightly lower for the largest CAS.

The right plot in Figure 9 shows the dependence on the T_{CutPNO} cut-off parameter. For very loose values, the discrepancy in accuracy for different spin states is apparent, especially for the larger CAS. However, it disappears with default and TightPNO settings of the cut-off. The method once again overestimates the correlation energy for the default value of T_{CutPairs} , but for tighter value $T_{\text{CutPairs}} = 10^{-5}$ it converges smoothly towards 100%.

Regarding the triples correction, the convergence behavior is similar as for oxo-Mn(Salen). The percentages of retrieved triples energy with respect to both T_{CutPairs} and T_{CutPNO} are shown in Figure 10. The DLPNO approximation for this correction is again the most sensitive to changes

TABLE III: Energy differences in kcal/mol between DLPNO-TCCSD and DLPNO-CCSD(T) calculations with different settings of cut-off parameters and equivalent canonical calculations on Fe(II)-porphyrin model in def2-SVP.

		CAS(8,12)		CAS(12,16)		CAS(32,34)	
		default	TightPNO	default	TightPNO	default	TightPNO
SD	T	0.85	3.01	1.10	2.27	1.42	3.28
	Q	0.69	2.41	0.73	2.04	2.16	3.40
	ΔE_{T-Q}	0.16	0.60	0.37	0.23	-0.74	-0.12
SD(T)	T	4.87	5.03	4.77	4.20	5.49	5.43
	Q	4.58	4.38	4.34	3.90	6.19	5.52
	ΔE_{T-Q}	0.29	0.65	0.43	0.30	-0.70	-0.09

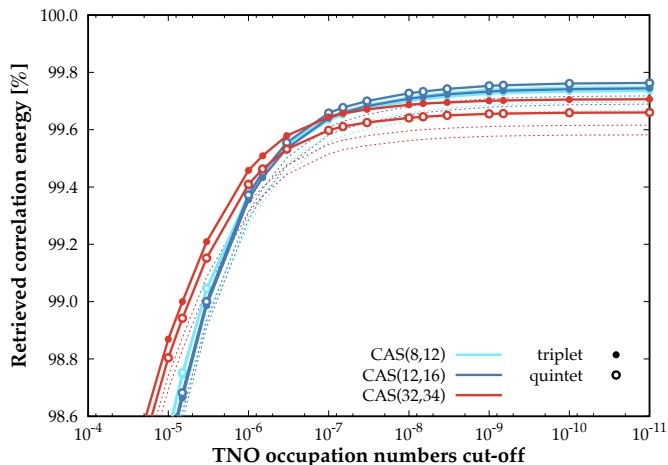


FIG. 11: The percentage of correlation energy of FeP in cc-pVDZ basis retrieved by DLPNO-TCCSD(T) with respect to canonical TCCSD(T) calculations as a function of cut-off for TNO occupation numbers T_{CutTNO} . The thin dashed lines represent the values for $T_{\text{CutPairs}} = 10^{-5}$.

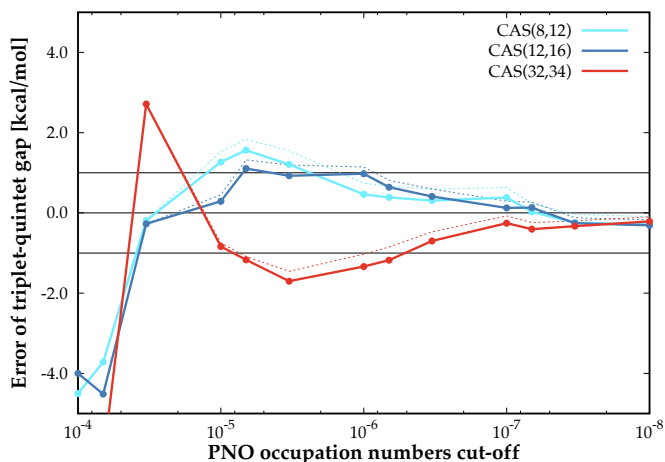


FIG. 12: The error of DLPNO-TCCSD(T) in singlet-triplet gap of FeP in cc-pVDZ basis with respect to canonical TCCSD(T) calculations as a function of cut-off for PNO occupation numbers T_{CutPNO} .

in T_{CutPNO} parameter, but shows clear convergence towards 100%. Dependence of total DLPNO correlation energy on T_{CutTNO} is shown in Figure 11.

Finally, we assess the accuracy of the triplet-quintet gap, which is the actual value of interest. Table III lists the energy differences between TCCSD, TCCSD(T) and their DLPNO versions. At the CCSD level, the errors for absolute energies grow with growing CAS. These errors are larger for the TightPNO settings, which is understandable given the method overshoots for looser T_{CutPairs} thresholds. However, the tighter cut-offs significantly improve the accuracy in energy of the triplet-quintet gap, with the exception of the smallest active space. Although the decrease in accuracy of the absolute energies is observed, once the perturbative triples correction is included, the errors in gaps are basically the same as in the CCSD case. Moreover, the dependence of the DLPNO error on T_{CutPNO} is presented in Figure 12. Even for the default cut-offs, the error is well under 1 kcal/mol and is even smaller for the TightPNO settings, with the previously discussed exception of CAS(8,12). Interestingly, the accuracy of the quintet state is consistently lower than for the triplet state for the largest CAS, while it is the opposite for the smaller active spaces.

V. CONCLUSIONS

We introduced a new version of DMRG-TCCSD method, which employs the domain-based local pair natural orbital approach. The method was implemented in ORCA and should be available in the next release, while the Budapest DMRG code is used for the DMRG part.

We performed several accuracy assessments of the method employing three systems, two of which have been previously studied by the canonical and LPNO versions of the TCCSD method.

For tetramethyleneethane, we were able to retrieve over 99.9% of the canonical correlation energy, while using the default settings of cut-off parameters, with negligible non-parallelity error with respect to its dihedral rotation. Also, the drawbacks present in the LPNO version were eliminated.

For oxo-Mn(Salen), the amount of retrieved correlation was dependent on the size of the used active space, ranging

from 99.8% for the larger CAS(28,27) to 99.9% for smaller CAS(28,22), which is an improvement about 0.2% with respect to LPNO-TCCSD. Using the default settings resulted in singlet-triplet gap being off by 0.5-0.6 kcal/mol and with tighter cut-offs only 0.3-0.4 kcal/mol compared to canonical calculation. These results are slightly worse than those of LPNO-TCCSD, which we believe is a consequence of a fortunate cancellation of errors in LPNO-TCCSD, since DLPNO-TCCSD are consistently better for the remaining two systems. Moreover, new implementation offers significantly better timing than the LPNO one.

For Fe(II)-porphyrin, the dependence on cut-off parameters was very similar as for oxo-Mn(Salen). With the default settings, we were able to retrieve more than 99.9% canonical correlation energy. Irrespective of the active space size, the method determined the triplet-quintet gap with error safely within the chemical accuracy of 1kcal/mol even with the default settings.

To summarize, we believe that DLPNO-DMRG-TCCSD(T) is a possible approach to treat systems with a moderate multireference character. In the near future, we would like to implement the DLPNO version of multireference TCCSD, which we hope to further enhance capabilities of this method.

ACKNOWLEDGMENT

We would like to thank Prof. Frank Neese for providing us with access to ORCA source code, as well as for helpful discussions, Dr. Frank Wennmohs for technical assistance with the ORCA code and Dr. Ondřej Demel for helpful discussions.

This work has been supported by the Czech Science Foundation (Grants No. 18-24563S, 16-12052S and 18-18940Y), the Hungarian National Research, Development and Innovation Office (NKFIH) through (Grant No. K120569), the Hungarian Quantum Technology National Excellence Program (Project No. 2017-1.2.1-NKP-2017-00001), by the Pacific Northwest National Laboratory (Contract No. 462268), and by the Czech Ministry of Education, Youth and Sports (Project No. LTAUSA17033 and the Large Infrastructures for Research, Experimental Development and Innovations project „IT4Innovations National Supercomputing Center – LM2015070“. Ö. Legeza acknowledges financial support from the Alexander von Humboldt foundation. Mutual visits with members of the Hungarian group have been partly supported by the Hungarian-Czech Joint Research Project MTA/19/04.

* jakub.lang@jh-inst.cas.cz

† andrej.antalik@jh-inst.cas.cz

‡ libor.veis@jh-inst.cas.cz

§ jan.brandejs@jh-inst.cas.cz

¶ jiri.brabec@jh-inst.cas.cz

** legeza.ors@wigner.mta.hu

†† jiri.pittner@jh-inst.cas.cz

¹ Čížek, J. On the Correlation Problem in Atomic and Molecular Systems. Calculation of Wavefunction Components in Ursell-Type Expansion Using Quantum-Field Theoretical Methods. *J. Chem. Phys.* **1966**, *45*, 4256–4266.

² Gauss, J. In *The Encyclopedia of Computational Chemistry*; v. R. Schleyer, P., Allinger, N. L., Clark, T., Gasteiger, J., Kollman, P. A., Schaefer III, H. F., Scheiner, P. R., Eds.; Wiley: Chichester, 1998; pp 615–636.

³ Raghavachari, K.; Trucks, G. W.; Pople, J. A.; Head-Gordon, M. A fifth-order perturbation comparison of electron correlation theories. *Chem. Phys. Lett.* **1989**, *157*, 479–483.

⁴ Bartlett, R. J.; Musiał, M. Coupled-cluster theory in quantum chemistry. *Rev. Mod. Phys.* **2007**, *79*, 291–352.

⁵ Tew, D. P.; Hättig, C.; Bachorz, R. A.; Klopper, W. In *Recent Progress in Coupled Cluster Methods*; Čársky, P., Paldus, J., Pittner, J., Eds.; Springer Science: New York, 2010; p 535.

⁶ Lyakh, D. I.; Musiał, M.; Lotrich, V. F.; Bartlett, R. J. Multireference Nature of Chemistry: The Coupled-Cluster View. *Chem. Rev.* **2012**, *112*, 182–243.

⁷ Li, X.; Paldus, J. Reduced multireference CCSD method: An effective approach to quasidegenerate states. *J. Chem. Phys.* **1997**, *107*, 6257–6269.

⁸ Li, X. Benchmark study of potential energies and vibrational levels using the reduced multireference coupled cluster method. The HF molecule. *J. Mol. Struct.: THEOCHEM*

2001, *547*, 69–81.

⁹ Li, X.; Paldus, J. Energy versus amplitude corrected coupled-cluster approaches. II. Breaking the triple bond. *J. Chem. Phys.* **2001**, *115*, 5774–5783.

¹⁰ Li, X.; Paldus, J. Energy versus amplitude corrected coupled-cluster approaches. I. *J. Chem. Phys.* **2001**, *115*, 5759–5773.

¹¹ Paldus, J.; Planelles, J. Valence bond corrected single reference coupled cluster approach. *Theor. Chim. Acta* **1994**, *89*, 13–31.

¹² Piecuch, P.; Tobol/a, R.; Paldus, J. Approximate account of connected quadruply excited clusters in single-reference coupled-cluster theory via cluster analysis of the projected unrestricted Hartree-Fock wave function. *Phys. Rev. A* **1996**, *54*, 1210–1241.

¹³ Li, X.; Peris, G.; Planelles, J.; Rajadall, F.; Paldus, J. Externally corrected singles and doubles coupled cluster methods for open-shell systems. *J. Chem. Phys.* **1997**, *107*, 90–98.

¹⁴ Kinoshita, T.; Hino, O.; Bartlett, R. J. Coupled-cluster method tailored by configuration interaction. *J. Chem. Phys.* **2005**, *123*, 074106.

¹⁵ Lyakh, D. I.; Lotrich, V. F.; Bartlett, R. J. The ‘tailored’ CCSD(T) description of the automerization of cyclobutadiene. *Chem. Phys. Lett.* **2011**, *501*, 166–171.

¹⁶ Melnichuk, A.; Bartlett, R. J. Relaxed active space: Fixing tailored-CC with high order coupled cluster. I. *J. Chem. Phys.* **2012**, *137*, 214103.

¹⁷ Melnichuk, A.; Bartlett, R. J. Relaxed active space: Fixing tailored-CC with high order coupled cluster. II. *J. Chem. Phys.* **2014**, *140*, 064113.

¹⁸ Piecuch, P.; Oliphant, N.; Adamowicz, L. A state-selective multireference coupled-cluster theory employing the single-reference formalism. *J. Chem. Phys.* **1993**, *99*, 1875–1900.

¹⁹ Piecuch, P.; Adamowicz, L. State-selective multireference

- coupled-cluster theory employing the single-reference formalism: Implementation and application to the H8 model system. *J. Chem. Phys.* **1994**, *100*, 5792–5809.
- ²⁰ Adamowicz, L.; Piecuch, P.; Ghose, K. B. The state-selective coupled cluster method for quasi-degenerate electronic states. *Mol. Phys.* **1998**, *94*, 225–234.
- ²¹ Piecuch, P. Active-space coupled-cluster methods. *Mol. Phys.* **2010**, *108*, 2987–3015.
- ²² Piecuch, P.; Kowalski, K.; Pimienta, I. S. O.; Mcguire, M. J. Recent advances in electronic structure theory: Method of moments of coupled-cluster equations and renormalized coupled-cluster approaches. *Int. Rev. Phys. Chem.* **2002**, *21*, 527–655.
- ²³ Piecuch, P.; Kowalski, K.; Pimienta, I. Method of Moments of Coupled-Cluster Equations: Externally Corrected Approaches Employing Configuration Interaction Wave Functions. *Int. J. Mol. Sci.* **2002**, *3*, 475–497.
- ²⁴ Kowalski, K.; Piecuch, P. Extension of the method of moments of coupled-cluster equations to excited states: The triples and quadruples corrections to the equation-of-motion coupled-cluster singles and doubles energies. *J. Chem. Phys.* **2002**, *116*, 7411–7423.
- ²⁵ łoch, M. W.; Lodriguito, M. D.; Piecuch†, P.; Gour, J. R. Two new classes of non-iterative coupled-cluster methods derived from the method of moments of coupled-cluster equations. *Mol. Phys.* **2006**, *104*, 2149–2172.
- ²⁶ Lodriguito, M. D.; Kowalski, K.; Włoch, M.; Piecuch, P. Non-iterative coupled-cluster methods employing multi-reference perturbation theory wave functions. *J. Mol. Struct.: THEOCHEM* **2006**, *771*, 89–104.
- ²⁷ Piecuch, P.; Kowalski, K.; Pimienta, I. S. O.; Fan, P.-D.; Lodriguito, M.; McGuire, M. J.; Kucharski, S. A.; Kuś, T.; Musiał, M. Method of moments of coupled-cluster equations: a new formalism for designing accurate electronic structure methods for ground and excited states. *Theor. Chem. Acc.* **2004**, *112*, 349–393.
- ²⁸ Kowalski, K.; Piecuch, P. New type of noniterative energy corrections for excited electronic states: Extension of the method of moments of coupled-cluster equations to the equation-of-motion coupled-cluster formalism. *J. Chem. Phys.* **2001**, *115*, 2966–2978.
- ²⁹ Kowalski, K.; Piecuch, P. The method of moments of coupled-cluster equations and the renormalized CCSD[T], CCSD(T), CCSD(TQ), and CCSDT(Q) approaches. *J. Chem. Phys.* **2000**, *113*, 18–35.
- ³⁰ Veis, L.; Antalík, A.; Brabec, J.; Neese, F.; Örs Legeza.; Pittner, J. Coupled Cluster Method with Single and Double Excitations Tailored by Matrix Product State Wave Functions. *J. Phys. Chem. Lett.* **2016**, *7*, 4072–4078.
- ³¹ Veis, L.; Antalík, A.; Brabec, J.; Neese, F.; Örs Legeza.; Pittner, J. Correction to Coupled Cluster Method with Single and Double Excitations Tailored by Matrix Product State Wave Functions. *J. Phys. Chem. Lett.* **2017**, *8*, 291–291.
- ³² Li, X.; Paldus, J. Reduced multireference CCSD method: An effective approach to quasidegenerate states. *J. Chem. Phys.* **1997**, *107*, 6257.
- ³³ Deustua, J. E.; Magoulas, I.; Shen, J.; Piecuch, P. Communication: Approaching exact quantum chemistry by cluster analysis of full configuration interaction quantum Monte Carlo wave functions. *J. Chem. Phys.* **2018**, *149*, 151101.
- ³⁴ White, S. R.; Noack, R. M. Real-space quantum renormalization groups. *Phys. Rev. Lett.* **1992**, *68*, 3487–3490.
- ³⁵ White, S. R. Density matrix formulation for quantum renormalization groups. *Phys. Rev. Lett.* **1992**, *69*, 2863–2866.
- ³⁶ White, S. R. Density-matrix algorithms for quantum renormalization groups. *Phys. Rev. B* **1993**, *48*, 10345–10356.
- ³⁷ White, S. R.; Martin, R. L. Ab initio quantum chemistry using the density matrix renormalization group. *J. Chem. Phys.* **1999**, *110*, 4127–4130.
- ³⁸ Chan, G. K.-L.; Head-Gordon, M. Highly correlated calculations with a polynomial cost algorithm: A study of the density matrix renormalization group. *J. Chem. Phys.* **2002**, *116*, 4462–4476.
- ³⁹ Legeza, O.; Röder, J.; Hess, B. A. Controlling the accuracy of the density-matrix renormalization-group method: The dynamical block state selection approach. *Phys. Rev. B* **2003**, *67*.
- ⁴⁰ Legeza, O.; Noack, R.; Sólyom, J.; Tincani, L. *Computational Many-Particle Physics*; Springer Berlin Heidelberg, pp 653–664.
- ⁴¹ Marti, K. H.; Reiher, M. The Density Matrix Renormalization Group Algorithm in Quantum Chemistry. *Z. Phys. Chem.* **2010**, *224*, 583–599.
- ⁴² Chan, G. K.-L.; Sharma, S. The Density Matrix Renormalization Group in Quantum Chemistry. *Annu. Rev. Phys. Chem.* **2011**, *62*, 465–481.
- ⁴³ Wouters, S.; Neck, D. V. The density matrix renormalization group for ab initio quantum chemistry. *Eur. Phys. J. D* **2014**, *68*.
- ⁴⁴ Szalay, S.; Pfeffer, M.; Murg, V.; Barcza, G.; Verstraete, F.; Schneider, R.; Örs Legeza, Tensor product methods and entanglement optimization for ab initio quantum chemistry. *Int. J. Quantum Chem.* **2015**, *115*, 1342–1391.
- ⁴⁵ Yanai, T.; Kurashige, Y.; Mizukami, W.; Chalupský, J.; Lan, T. N.; Saitow, M. Density matrix renormalization group for ab initio calculations and associated dynamic correlation methods: A review of theory and applications. *Int. J. Quantum Chem.* **2014**, *115*, 283–299.
- ⁴⁶ Kurashige, Y.; Yanai, T. Second-order perturbation theory with a density matrix renormalization group self-consistent field reference function: Theory and application to the study of chromium dimer. *J. Chem. Phys.* **2011**, *135*, 094104.
- ⁴⁷ Freitag, L.; Knecht, S.; Angeli, C.; Reiher, M. Multireference Perturbation Theory with Cholesky Decomposition for the Density Matrix Renormalization Group. *J. Chem. Theory Comput.* **2017**, *13*, 451–459.
- ⁴⁸ Saitow, M.; Kurashige, Y.; Yanai, T. Multireference configuration interaction theory using cumulant reconstruction with internal contraction of density matrix renormalization group wave function. *J. Chem. Phys.* **2013**, *139*, 044118.
- ⁴⁹ Neuscamman, E.; Yanai, T.; Chan, G. K.-L. A review of canonical transformation theory. *Int. Rev. Phys. Chem.* **2010**, *29*, 231–271.
- ⁵⁰ Sharma, S.; Chan, G. K.-L. Communication: A flexible multi-reference perturbation theory by minimizing the Hylleraas functional with matrix product states. *J. Chem. Phys.* **2014**, *141*, 111101.
- ⁵¹ Sharma, P.; Bernales, V.; Knecht, S.; Truhlar, D. G.; Gagliardi, L. Density matrix renormalization group pair-density functional theory (DMRG-PDFT): singlet–triplet gaps in polyacenes and polyacetylenes. *Chem. Sci.* **2019**, *10*, 1716–1723.
- ⁵² Faulstich, F. M.; Laestadius, A.; Örs Legeza.; Schneider, R.; Kvaal, S. Analysis of the Tailored Coupled-Cluster Method in Quantum Chemistry. *SIAM J. Numer. Anal.* **2019**, *57*, 2579–2607.
- ⁵³ Faulstich, F. M.; Máté, M.; Laestadius, A.; Csirik, M. A.; Veis, L.; Antalík, A.; Brabec, J.; Schneider, R.; Pittner, J.;

- Kvaal, S.; Örs Legeza, Numerical and Theoretical Aspects of the DMRG-TCC Method Exemplified by the Nitrogen Dimer. *J. Chem. Theory Comput.* **2019**, *15*, 2206–2220.
- ⁵⁴ Veis, L.; Antalík, A.; Örs Legeza,.; Alavi, A.; Pittner, J. The Intricate Case of Tetramethylethane: A Full Configuration Interaction Quantum Monte Carlo Benchmark and Multireference Coupled Cluster Studies. *J. Chem. Theory Comput.* **2018**, *14*, 2439–2445.
- ⁵⁵ Pulay, P. Localizability of dynamic electron correlation. *Chem. Phys. Lett.* **1983**, *100*, 151–154.
- ⁵⁶ Sæbø, S.; Pulay, P. Local configuration interaction: An efficient approach for larger molecules. *Chem. Phys. Lett.* **1985**, *113*, 13–18.
- ⁵⁷ Foster, J. M.; Boys, S. F. Canonical Configurational Interaction Procedure. *Rev. Mod. Phys.* **1960**, *32*, 300–302.
- ⁵⁸ Pipek, J.; Mezey, P. G. A fast intrinsic localization procedure applicable for ab initio and semiempirical linear combination of atomic orbital wave functions. *J. Chem. Phys.* **1989**, *90*, 4916–4926.
- ⁵⁹ Knizia, G. Intrinsic Atomic Orbitals: An Unbiased Bridge between Quantum Theory and Chemical Concepts. *J. Chem. Theory Comput.* **2013**, *9*, 4834–4843.
- ⁶⁰ Sæbø, S.; Pulay, P. Fourth-order Møller–Plessett perturbation theory in the local correlation treatment. I. Method. *J. Chem. Phys.* **1987**, *86*, 914–922.
- ⁶¹ Sæbø, S.; Pulay, P. The local correlation treatment. II. Implementation and tests. *J. Chem. Phys.* **1988**, *88*, 1884–1890.
- ⁶² Hampel, C.; Werner, H.-J. Local treatment of electron correlation in coupled cluster theory. *J. Chem. Phys.* **1996**, *104*, 6286–6297.
- ⁶³ Schütz, M.; Werner, H.-J. Low-order scaling local electron correlation methods. IV. Linear scaling local coupled-cluster (LCCSD). *J. Chem. Phys.* **2001**, *114*, 661.
- ⁶⁴ Schütz, M. A new, fast, semi-direct implementation of linear scaling local coupled cluster theory. *Phys. Chem. Chem. Phys.* **2002**, *4*, 3941–3947.
- ⁶⁵ Werner, H.-J.; Schütz, M. An efficient local coupled cluster method for accurate thermochemistry of large systems. *J. Chem. Phys.* **2011**, *135*, 144116.
- ⁶⁶ Schütz, M. Low-order scaling local electron correlation methods. V. Connected triples beyond (T): Linear scaling local CCSDT-1b. *J. Chem. Phys.* **2002**, *116*, 8772–8785.
- ⁶⁷ Kristensen, K.; Ziolkowski, M.; Jansik, B.; Kjær-gaard, T.; Jørgensen, P. A Locality Analysis of the Divide–Expand–Consolidate Coupled Cluster Amplitude Equations. *J. Chem. Theory Comput.* **2011**, *7*, 1677–1694.
- ⁶⁸ Høyvik, I.-M.; Kristensen, K.; Jansik, B.; Jørgensen, P. The divide-expand-consolidate family of coupled cluster methods: Numerical illustrations using second order Møller–Plesset perturbation theory. *J. Chem. Phys.* **2012**, *136*, 014105.
- ⁶⁹ Kobayashi, M.; Nakai, H. Extension of linear-scaling divide-and-conquer-based correlation method to coupled cluster theory with singles and doubles excitations. *J. Chem. Phys.* **2008**, *129*, 044103.
- ⁷⁰ Stoll, H. The correlation energy of crystalline silicon. *Chem. Phys. Lett.* **1992**, *191*, 548–552.
- ⁷¹ Rolik, Z.; Kállay, M. A general-order local coupled-cluster method based on the cluster-in-molecule approach. *J. Chem. Phys.* **2011**, *135*, 104111.
- ⁷² Fedorov, D. G.; Kitaura, K. Coupled-cluster theory based upon the fragment molecular-orbital method. *J. Chem. Phys.* **2005**, *123*, 134103.
- ⁷³ Li, S.; Ma, J.; Jiang, Y. Linear scaling local correlation approach for solving the coupled cluster equations of large systems. *J. Comput. Chem.* **2001**, *23*, 237–244.
- ⁷⁴ Edmiston, C.; Krauss, M. Configuration-Interaction Calculation of H3 and H2. *J. Chem. Phys.* **1965**, *42*, 1119–1120.
- ⁷⁵ Meyer, W. Ionization energies of water from PNO-CI calculations. *Int. J. Quantum Chem.* **1971**, *5*, 341–348.
- ⁷⁶ Meyer, W. PNO-CI and CEPA studies of electron correlation effects. *Theor. Chim. Acta* **1974**, *35*, 277–292.
- ⁷⁷ Werner, H.-J.; Meyer, W. PNO-CI and PNO-CEPA studies of electron correlation effects. *Mol. Phys.* **1976**, *31*, 855–872.
- ⁷⁸ Botschwina, P.; Meyer, W. PNO-CEPA calculation of collinear potential energy barriers for thermoneutral exchange reactions. *Chem. Phys.* **1977**, *20*, 43–52.
- ⁷⁹ Rosmus, P.; Meyer, W. PNO-CI and CEPA studies of electron correlation effects. VI. Electron affinities of the first-row and second-row diatomic hydrides and the spectroscopic constants of their negative ions. *J. Chem. Phys.* **1978**, *69*, 2745.
- ⁸⁰ Ahlrichs, R.; Kutzelnigg, W. Ab initio calculations on small hydrides including electron correlation. *Theor. Chim. Acta* **1968**, *10*, 377–387.
- ⁸¹ Ahlrichs, R.; Driessler, F.; Lischka, H.; Staemmler, V.; Kutzelnigg, W. PNO-CI (pair natural orbital configuration interaction) and CEPA-PNO (coupled electron pair approximation with pair natural orbitals) calculations of molecular systems. II. The molecules BeH₂, BH, BH₃, CH₄, CH₃⁻, NH₃ (planar and pyramidal), H₂O, OH₃⁺, HF and the Ne atom. *J. Chem. Phys.* **1975**, *62*, 1235–1247.
- ⁸² Neese, F.; Wennmohs, F.; Hansen, A. Efficient and accurate local approximations to coupled-electron pair approaches: An attempt to revive the pair natural orbital method. *J. Chem. Phys.* **2009**, *130*, 114108.
- ⁸³ Neese, F.; Hansen, A.; Liakos, D. G. Efficient and accurate approximations to the local coupled cluster singles doubles method using a truncated pair natural orbital basis. *J. Chem. Phys.* **2009**, *131*, 064103.
- ⁸⁴ Hansen, A.; Liakos, D. G.; Neese, F. Efficient and accurate local single reference correlation methods for high-spin open-shell molecules using pair natural orbitals. *J. Chem. Phys.* **2011**, *135*, 214102.
- ⁸⁵ Huntington, L. M. J.; Hansen, A.; Neese, F.; Nooijen, M. Accurate thermochemistry from a parameterized coupled-cluster singles and doubles model and a local pair natural orbital based implementation for applications to larger systems. *J. Chem. Phys.* **2012**, *136*, 064101.
- ⁸⁶ Riplinger, C.; Neese, F. An efficient and near linear scaling pair natural orbital based local coupled cluster method. *J. Chem. Phys.* **2013**, *138*, 034106.
- ⁸⁷ Pinski, P.; Riplinger, C.; Valeev, E. F.; Neese, F. Sparse maps—A systematic infrastructure for reduced-scaling electronic structure methods. I. An efficient and simple linear scaling local MP2 method that uses an intermediate basis of pair natural orbitals. *J. Chem. Phys.* **2015**, *143*, 034108.
- ⁸⁸ Riplinger, C.; Pinski, P.; Becker, U.; Valeev, E. F.; Neese, F. Sparse maps—A systematic infrastructure for reduced-scaling electronic structure methods. II. Linear scaling domain based pair natural orbital coupled cluster theory. *J. Chem. Phys.* **2016**, *144*, 024109.
- ⁸⁹ Saitow, M.; Becker, U.; Riplinger, C.; Valeev, E. F.; Neese, F. A new near-linear scaling, efficient and accurate, open-shell domain-based local pair natural orbital coupled cluster singles and doubles theory. *J. Chem. Phys.* **2017**, *146*, 164105.

- 90 Werner, H.-J.; Knizia, G.; Krause, C.; Schwilk, M.; Dornbach, M. Scalable Electron Correlation Methods I: PNO-LMP2 with Linear Scaling in the Molecular Size and Near-Inverse-Linear Scaling in the Number of Processors. *J. Chem. Theory Comput.* **2015**, *11*, 484–507.
- 91 Menezes, F.; Kats, D.; Werner, H.-J. Local complete active space second-order perturbation theory using pair natural orbitals (PNO-CASPT2). *J. Chem. Phys.* **2016**, *145*, 124115.
- 92 Schwilk, M.; Ma, Q.; Köppl, C.; Werner, H.-J. Scalable Electron Correlation Methods. 3. Efficient and Accurate Parallel Local Coupled Cluster with Pair Natural Orbitals (PNO-LCCSD). *J. Chem. Theory Comput.* **2017**, *13*, 3650–3675.
- 93 Tew, D. P.; Helmich, B.; Hättig, C. Local explicitly correlated second-order Møller–Plesset perturbation theory with pair natural orbitals. *J. Chem. Phys.* **2011**, *135*, 074107.
- 94 Helmich, B.; Hättig, C. A pair natural orbital implementation of the coupled cluster model CC2 for excitation energies. *J. Chem. Phys.* **2013**, *139*, 084114.
- 95 Schmitz, G.; Helmich, B.; Hättig, C. A scaling PNO–MP2 method using a hybrid OSV–PNO approach with an iterative direct generation of OSVs†. *Mol. Phys.* **2013**, *111*, 2463–2476.
- 96 Guo, Y.; Sivalingam, K.; Valeev, E. F.; Neese, F. SparseMaps—A systematic infrastructure for reduced-scaling electronic structure methods. III. Linear-scaling multireference domain-based pair natural orbital N-electron valence perturbation theory. *J. Chem. Phys.* **2016**, *144*, 094111.
- 97 Antony, J.; Grimme, S.; Liakos, D. G.; Neese, F. Protein–Ligand Interaction Energies with Dispersion Corrected Density Functional Theory and High-Level Wave Function Based Methods. *J. Phys. Chem. A* **2011**, *115*, 11210–11220.
- 98 Anoop, A.; Thiel, W.; Neese, F. A Local Pair Natural Orbital Coupled Cluster Study of Rh Catalyzed Asymmetric Olefin Hydrogenation. *J. Chem. Theory Comput.* **2010**, *6*, 3137–3144.
- 99 Liakos, D. G.; Neese, F. Interplay of Correlation and Relativistic Effects in Correlated Calculations on Transition-Metal Complexes: The $(\text{Cu}_2\text{O}_2)^{2+}$ Core Revisited. *J. Chem. Theory Comput.* **2011**, *7*, 1511–1523.
- 100 Zade, S. S.; Zamoshchik, N.; Reddy, A. R.; Fridman-Marueli, G.; Sheberla, D.; Bendikov, M. Products and Mechanism of Acene Dimerization. A Computational Study. *J. Am. Chem. Soc.* **2011**, *133*, 10803–10816.
- 101 Kubas, A.; Bräse, S.; Fink, K. Theoretical Approach Towards the Understanding of Asymmetric Additions of Dialkylzinc to Enals and Iminals Catalysed by [2.2]Paracyclophane-Based N, O-Ligands. *Chem.: Eur. J.* **2012**, *18*, 8377–8385.
- 102 Ashtari, M.; Cann, N. Proline-based chiral stationary phases: A molecular dynamics study of the interfacial structure. *J. Chromatogr. A* **2011**, *1218*, 6331–6347.
- 103 Zhang, J.; Dolg, M. Dispersion Interaction Stabilizes Sterically Hindered Double Fullerenes. *Chem.: Eur. J.* **2014**, *20*, 13909–13912.
- 104 Minenkov, Y.; Chermak, E.; Cavallo, L. Accuracy of DLPNO–CCSD(T) Method for Noncovalent Bond Dissociation Enthalpies from Coinage Metal Cation Complexes. *J. Chem. Theory Comput.* **2015**, *11*, 4664–4676.
- 105 Sparta, M.; Neese, F. Chemical applications carried out by local pair natural orbital based coupled-cluster methods. *Chem. Soc. Rev.* **2014**, *43*, 5032–5041.
- 106 Liakos, D. G.; Sparta, M.; Kesharwani, M. K.; Martin, J. M. L.; Neese, F. Exploring the Accuracy Limits of Local Pair Natural Orbital Coupled-Cluster Theory. *J. Chem. Theory Comput.* **2015**, *11*, 1525–1539.
- 107 Demel, O.; Pittner, J.; Neese, F. A Local Pair Natural Orbital-Based Multireference Mukherjee’s Coupled Cluster Method. *J. Chem. Theory Comput.* **2015**, *11*, 3104–3114.
- 108 Lang, J.; Švaňa, M.; Demel, O.; Brabec, J.; Kedžuch, S.; Noga, J.; Kowalski, K.; Pittner, J. A MRCC study of the isomerisation of cyclopropane. *Mol. Phys.* **2017**, *115*, 2743–2754.
- 109 Brabec, J.; Lang, J.; Saitow, M.; Pittner, J.; Neese, F.; Demel, O. Domain-Based Local Pair Natural Orbital Version of Mukherjee’s State-Specific Coupled Cluster Method. *J. Chem. Theory Comput.* **2018**, *14*, 1370–1382.
- 110 Lang, J.; Brabec, J.; Saitow, M.; Pittner, J.; Neese, F.; Demel, O. Perturbative triples correction to domain-based local pair natural orbital variants of Mukherjee’s state specific coupled cluster method. *Phys. Chem. Chem. Phys.* **2019**, *21*, 5022–5038.
- 111 Antalík, A.; Veis, L.; Brabec, J.; Demel, O.; Örs Legeza.; Pittner, J. Toward the efficient local tailored coupled cluster approximation and the peculiar case of oxo-Mn(Salen). *J. Chem. Phys.* **2019**, *151*, 084112.
- 112 Kowalski, K. Properties of coupled-cluster equations originating in excitation sub-algebras. *The Journal of Chemical Physics* **2018**, *148*, 094104.
- 113 Bauman, N. P.; Bylaska, E. J.; Krishnamoorthy, S.; Low, G. H.; Wiebe, N.; Granade, C. E.; Roetteler, M.; Troyer, M.; Kowalski, K. Downfolding of many-body Hamiltonians using active-space models: Extension of the subsystem embedding sub-algebras approach to unitary coupled cluster formalisms. *The Journal of Chemical Physics* **2019**, *151*, 014107.
- 114 Moritz, G.; Reiher, M. Decomposition of density matrix renormalization group states into a Slater determinant basis. *J. Chem. Phys.* **2007**, *126*, 244109.
- 115 Boguslawski, K.; Marti, K. H.; Reiher, M. Construction of CASCI-type wave functions for very large active spaces. *J. Chem. Phys.* **2011**, *134*, 224101.
- 116 Neese, F. The ORCA program system. *Wiley Interdiscip. Rev. Comput. Mol. Sci.* **2011**, *2*, 73–78.
- 117 Olivares-Amaya, R.; Hu, W.; Nakatani, N.; Sharma, S.; Yang, J.; Chan, G. K.-L. The ab-initio density matrix renormalization group in practice. *J. Chem. Phys.* **2015**, *142*, 034102.
- 118 Adler, T. B.; Werner, H.-J. An explicitly correlated local coupled cluster method for calculations of large molecules close to the basis set limit. *J. Chem. Phys.* **2011**, *135*, 144117.
- 119 Adler, T. B.; Werner, H.-J. Local explicitly correlated coupled-cluster methods: Efficient removal of the basis set incompleteness and domain errors. *J. Chem. Phys.* **2009**, *130*, 241101.
- 120 Riplinger, C.; Sandhoefer, B.; Hansen, A.; Neese, F. Natural triple excitations in local coupled cluster calculations with pair natural orbitals. *J. Chem. Phys.* **2013**, *139*, 134101.
- 121 Guo, Y.; Riplinger, C.; Becker, U.; Liakos, D. G.; Minenkov, Y.; Cavallo, L.; Neese, F. Communication: An improved linear scaling perturbative triples correction for the domain based local pair-natural orbital based singles and doubles coupled cluster method [DLPNO-CCSD(T)]. *J. Chem. Phys.* **2018**, *148*, 011101.
- 122 Legeza, Ö.; Veis, L.; Mosoni, T. QC-DMRG-Budapest, a program for quantum chemical DMRG calculations.

- ¹²³ Barcza, G.; Legeza, O.; Marti, K. H.; Reiher, M. Quantum-information analysis of electronic states of different molecular structures. *Phys. Rev. A* **2011**, *83*.
- ¹²⁴ Fertitta, E.; Paulus, B.; Barcza, G.; Legeza, O. Investigation of metal-insulator-like transition through thead initio-density matrix renormalization group approach. *Phys. Rev. B* **2014**, *90*.
- ¹²⁵ Legeza, O.; Sólyom, J. Optimizing the density-matrix renormalization group method using quantum information entropy. *Phys. Rev. B* **2003**, *68*, 195116.
- ¹²⁶ Legeza, O.; Sólyom, J. Quantum data compression, quantum information generation, and the density-matrix renormalization-group method. *Phys. Rev. B* **2004**, *70*, 205118.
- ¹²⁷ Bross, D. H.; Hill, J. G.; Werner, H.-J.; Peterson, K. A. Explicitly correlated composite thermochemistry of transition metal species. *J. Chem. Phys.* **2013**, *139*, 094302.
- ¹²⁸ Ivanic, J.; Collins, J. R.; Burt, S. K. Theoretical Study of the Low Lying Electronic States of oxoX(salen) (X = Mn, Mn-, Fe, and Cr-) Complexes. *J. Phys. Chem. A* **2004**, *108*, 2314–2323.
- ¹²⁹ Ghosh, D.; Hachmann, J.; Yanai, T.; Chan, G. K.-L. Orbital optimization in the density matrix renormalization group, with applications to polyenes and β -carotene. *J. Chem. Phys.* **2008**, *128*, 144117.
- ¹³⁰ Zgid, D.; Nooijen, M. The density matrix renormalization group self-consistent field method: Orbital optimization with the density matrix renormalization group method in the active space. *J. Chem. Phys.* **2008**, *128*, 144116.
- ¹³¹ Yanai, T.; Kurashige, Y.; Ghosh, D.; Chan, G. K.-L. Accelerating convergence in iterative solution for large-scale complete active space self-consistent-field calculations. *Int. J. Quantum Chem.* **2009**, *109*, 2178–2190.
- ¹³² Dunning, T. H. Gaussian basis sets for use in correlated molecular calculations. I. The atoms boron through neon and hydrogen. *J. Chem. Phys.* **1989**, *90*, 1007–1023.
- ¹³³ Woon, D. E.; Dunning, T. H. Gaussian basis sets for use in correlated molecular calculations. III. The atoms aluminum through argon. *J. Chem. Phys.* **1993**, *98*, 1358–1371.
- ¹³⁴ Balabanov, N. B.; Peterson, K. A. Systematically convergent basis sets for transition metals. I. All-electron correlation consistent basis sets for the 3d elements Sc–Zn. *J. Chem. Phys.* **2005**, *123*, 064107.
- ¹³⁵ Weigend, F.; Köhn, A.; Hättig, C. Efficient use of the correlation consistent basis sets in resolution of the identity MP2 calculations. *J. Chem. Phys.* **2002**, *116*, 3175–3183.
- ¹³⁶ Manni, G. L.; Alavi, A. Understanding the Mechanism Stabilizing Intermediate Spin States in Fe(II)-Porphyrin. *J. Phys. Chem. A* **2018**, *122*, 4935–4947.
- ¹³⁷ Weigend, F.; Ahlrichs, R. Balanced basis sets of split valence, triple zeta valence and quadruple zeta valence quality for H to Rn: Design and assessment of accuracy. *Phys. Chem. Chem. Phys.* **2005**, *7*, 3297.
- ¹³⁸ Hellweg, A.; Hättig, C.; Höfener, S.; Klopper, W. Optimized accurate auxiliary basis sets for RI-MP2 and RI-CC2 calculations for the atoms Rb to Rn. *Theor. Chem. Acc.* **2007**, *117*, 587–597.
- ¹³⁹ Pittner, J.; Nachtigall, P.; Čársky, P.; Hubač, I. State-Specific Brillouin-Wigner Multireference Coupled Cluster Study of the Singlet-Triplet Separation in the Tetramethyleneethane Diradical. *J. Phys. Chem. A* **2001**, *105*, 1354–1356.
- ¹⁴⁰ Bhaskaran-Nair, K.; Demel, O.; Šmydke, J.; Pittner, J. Multireference state-specific Mukherjee’s coupled cluster method with noniterative triexcitations using uncoupled approximation. *J. Chem. Phys.* **2011**, *134*, 154106.
- ¹⁴¹ Chattopadhyay, S.; Chaudhuri, R. K.; Mahapatra, U. S. Ab Initio Multireference Investigation of Disjoint Diradicals: Singlet versus Triplet Ground States. *ChemPhysChem* **2011**, *12*, 2791–2797.
- ¹⁴² Pozun, Z. D.; Su, X.; Jordan, K. D. Establishing the Ground State of the Disjoint Diradical Tetramethyleneethane with Quantum Monte Carlo. *J. Am. Chem. Soc.* **2013**, *135*, 13862–13869.
- ¹⁴³ Zhang, W.; Loebach, J. L.; Wilson, S. R.; Jacobsen, E. N. Enantioselective epoxidation of unfunctionalized olefins catalyzed by salen manganese complexes. *J. Am. Chem. Soc.* **1990**, *112*, 2801–2803.
- ¹⁴⁴ Irie, R.; Noda, K.; Ito, Y.; Matsumoto, N.; Katsuki, T. Catalytic asymmetric epoxidation of unfunctionalized olefins. *Tetrahedron Lett.* **1990**, *31*, 7345–7348.
- ¹⁴⁵ Sears, J. S.; Sherrill, C. D. The electronic structure of oxo-Mn(salen): Single-reference and multireference approaches. *J. Chem. Phys.* **2006**, *124*, 144314.
- ¹⁴⁶ Ma, D.; Manni, G. L.; Gagliardi, L. The generalized active space concept in multiconfigurational self-consistent field methods. *J. Chem. Phys.* **2011**, *135*, 044128.
- ¹⁴⁷ Wouters, S.; Bogaerts, T.; Voort, P. V. D.; Speybroeck, V. V.; Neck, D. V. Communication: DMRG-SCF study of the singlet, triplet, and quintet states of oxo-Mn(Salen). *J. Chem. Phys.* **2014**, *140*, 241103.
- ¹⁴⁸ Stein, C. J.; Reiher, M. Automated Selection of Active Orbital Spaces. *J. Chem. Theory Comput.* **2016**, *12*, 1760–1771.
- ¹⁴⁹ Sharma, S.; Knizia, G.; Guo, S.; Alavi, A. Combining Internally Contracted States and Matrix Product States To Perform Multireference Perturbation Theory. *J. Chem. Theory Comput.* **2017**, *13*, 488–498.
- ¹⁵⁰ Manni, G. L.; Kats, D.; Tew, D. P.; Alavi, A. Role of Valence and Semicore Electron Correlation on Spin Gaps in Fe(II)-Porphyrins. *J. Chem. Theory Comput.* **2019**, *15*, 1492–1497.